



HAL
open science

Computed Tomography to Ultrasound 2D image registration evaluation for atrial fibrillation treatment

Zulma Sandoval, Jean-Louis Dillenseger

► **To cite this version:**

Zulma Sandoval, Jean-Louis Dillenseger. Computed Tomography to Ultrasound 2D image registration evaluation for atrial fibrillation treatment. Computing in Cardiology Conference (CinC), 2013, Sep 2013, Zaragoza, Spain. pp.245-248. inserm-00935317

HAL Id: inserm-00935317

<https://inserm.hal.science/inserm-00935317>

Submitted on 23 Jan 2014

HAL is a multi-disciplinary open access archive for the deposit and dissemination of scientific research documents, whether they are published or not. The documents may come from teaching and research institutions in France or abroad, or from public or private research centers.

L'archive ouverte pluridisciplinaire **HAL**, est destinée au dépôt et à la diffusion de documents scientifiques de niveau recherche, publiés ou non, émanant des établissements d'enseignement et de recherche français ou étrangers, des laboratoires publics ou privés.

Evaluation of Computed Tomography to Ultrasound 2D Image Registration for Atrial Fibrillation Treatment

Zulma L Sandoval, Jean-Louis Dillenseger

INSERM, URM1099, Rennes, France
Université de Rennes 1, LTSI, Rennes, France

Abstract

This work aims to evaluate intensity-based similarity measures used in rigid or elastic registration techniques to align preoperative computed tomography (CT) and transesophageal ultrasound (US) images of the left atrium and the pulmonary veins, in order to guide high intensity focused ultrasound (HIFU) ablation therapy in patients with atrial fibrillation. The evaluation of the registration techniques has four steps: (i) design of anatomical 2D models including the left atrium and the pulmonary veins from the cryosections of the Visible Human Project, (ii) application of a known rigid/nonrigid transformation in order to produce a gold standard, (iii) creation of a pair of synthetic US and CT images, (iv) estimation of the transformation by rigid/elastic registration of the simulated images and comparison with the gold standard. The performance of eight similarity measures was evaluated for rigid registration: mutual information (MI), normalized mutual information (NMI), entropy correlation coefficient (ECC), joint entropy (H), point similarity measure based on MI (PSMI), energy of histogram (E), correlation ratio (CoR) and Woods criterion (WC). The evaluation protocol estimated the accuracy and the global optimization tendency around the gold standard. For the elastic registration the level of accuracy obtained using MI and NMI was measured.

1. Introduction

Ablation procedures have proven to be some of the most effective methods in treating atrial fibrillation [1]. These procedures aim to establish a line of lesions around the pulmonary veins in order to block trigger points of atrial fibrillation. Ultrasound-guided HIFU is a minimally-invasive alternative to other ablation techniques [2]. In this procedure, the ablation path is defined in a preoperative stage on 3D cine CT scans. The ablation itself is performed under 2D ultrasound (US) guidance. The 2D-3D registration of intra-operative US images to the pre-operative CT images is then needed in order to transfer and follow the ablation

path in the pre-operative context.

The registration procedure of two images of the same scene acquired at different times or from different points of view and/or by different sensors, aims to align them into a common referential. Usually, one image is fixed as a reference and the other is moved and compared with it. The registration procedure usually consists of 1) applying a geometric transformation to the moving image, 2) comparing similarities between the two images and 3) optimizing the geometric transformation parameters in order to maximize the similarity between the two images.

An intensity-based cardiac US to cardiac CT image rigid registration method has been described in [3]. The authors of this paper proposed a spatio-temporal registration of the beating heart using mutual information (MI) metric to drive the spatial alignment. This technique has been improved by performing an intensity-based registration on only the relevant features of the US image after median filtering and low intensity thresholding [4]. The question of MI validity thus arises. In CT images, tissues are characterized by intensities distribution. However, in US images, each tissue is inherently characterized by a specific spatial distribution of speckle rather than a specific distribution of gray levels. Therefore, the use of an intensity-based SM in a multimodality image registration problem involving US images is still an open question. Beside MI, other intensity-based SMs have also been proposed in the literature. Some of these metrics could be more adequate than MI in driving the registration in all clinical context.

Moreover, rigid registration seems not to be the most appropriate in our beating hearth context. The evaluation of SM should also be performed in an elastic registration context.

This document is structured as follows: the geometrical transformation and the similarity measures used in the evaluation are described section 2 and section 3, respectively. In section 4, the evaluation protocol is defined. The experimental results are shown and discussed in section 5.

2. Geometrical transformations

Image registration can be formulated as an optimization problem in which the cost function C is minimized as:

$$\widehat{T}_\mu = \arg \min_{T_\mu} C(T_\mu; I_F, I_M) \quad (1)$$

where T_μ indicates the parametrized geometrical transformation, I_F is the fixed image and I_M is the moving image. The vector μ contains the values of the transformation that we want to optimize in order to maximize similarity between the two images. In this paper we will explore two 2D transformations: Rigid (Eq. 2) and Elastic B-splines based (Eq. 3).

$$T_\mu = T(\phi, d_x, d_y) = \begin{bmatrix} \cos\phi & -\sin\phi & d_x \\ \sin\phi & \cos\phi & d_y \\ 0 & 0 & 1 \end{bmatrix} \quad (2)$$

with ϕ = rotation, d_x = translation in x and d_y = translation in y directions.

$$T_\mu(\mathbf{x}) = \mathbf{x} + \sum_{\mathbf{x}_k \in N_x} p_k \beta^3 \left(\frac{\mathbf{x} - \mathbf{x}_k}{\sigma} \right) \quad (3)$$

with \mathbf{x}_k the control points, $\beta^3()$ the cubic multidimensional B-spline polynomial [5], p_k the B-spline coefficient vectors, σ the B-spline control points spacing, and N_x the set of all control points within the compact support of the B-spline at \mathbf{x} .

3. Similarity measures

The similarity measures are cost functions that measure the similarity between the I_F and the transformed I_M . Ideally, the SM has an optimum at the set of parameters that best align the moving image, and values that decrease monotonically with the distance to the optimum. Similarity measure is the critical aspect of an intensity based registration. Its variational behavior (e.g. presence of global minima,...) around the global optimum impacts directly the optimization step and the registration quality.

In this paper, eight intensity-based SMs are evaluated. Six of these SMs use the information from the histogram of images while two of them use the spatial information and intensity values. They are: mutual information (MI) [6], normalized mutual information (NMI) [7], entropy correlation coefficient (ECC) [6], joint entropy (H) [6], point similarity measure based on MI (PSMI) [8], histogram energy (E) [9], correlation ratio (CoR) [10] and Woods criterion (WC) [11].

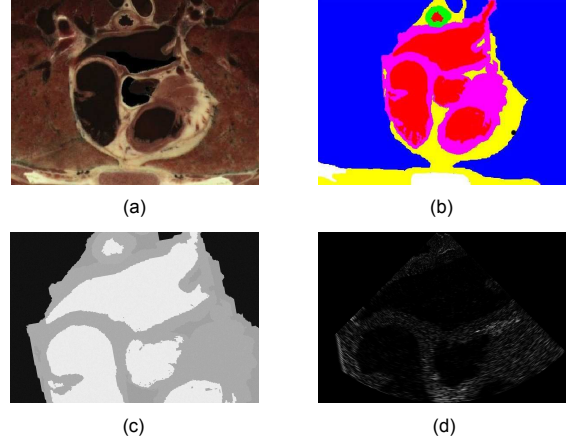


Figure 1. Images used for evaluation. Left atrium and pulmonary veins phantom images: cryosection of male human thorax (a); segmented and labeled into six different types of tissues (b); corresponding simulated CT (c) and US (d) images.

4. Image registration evaluation

The evaluation of the registration techniques has four steps: (i) design of anatomical 2D models including the left atrium and the pulmonary veins from the cryosections of the Visible Human Project (male and female), (ii) application of a known rigid/nonrigid transformation in order to produce a gold standard, (iii) creation of a pair of synthetic US images and CT slices, (iv) estimation of the transformation by rigid/elastic registration of the simulated images and comparison with the gold standard.

4.1. Anatomical models and synthetic US and CT images

We create a set of four synthetic phantom images of the left atrium and pulmonary veins (LAPVs). For these, we first pick four slices from the male and female cryosections of the Visible Human Project ¹. As an example, Fig. 1-(a) shows a slice from the male dataset. These LAPVs images were segmented and labeled into six types of tissues: air, fat, bone, muscle, water and blood (Fig. 1-(b)).

Synthetic CT images were obtained by applying the Hounsfield value corresponding to the type of tissue modulated by Gaussian noise (Fig. 1-(c)).

For simulating US images we characterized each tissue by its acoustical impedance and a spatial distribution of speckle. This information is set as an input to an US image simulator [12] (Fig. 1-(d)).

¹http://www.nlm.nih.gov/research/visible/visible_gallery.html

Table 1. Value of the ACC(mm), RON ($10^6/mm$), NOM, CR(mm) and DO ($1/mm$) properties for the eight similarity measures evaluated on: the raw LAPV image (RI) and the preprocessed LAPV image (PI). Best values are bolded.

| | ACC | | RON | | NOM | | CR | | DO | |
|------|-------------|----------|------------|------------|-----------|-----------|--------------|--------------|-----------|-----------|
| | RI | PI | RI | PI | RI | PI | RI | PI | RI | PI |
| MI | 0.17 | 0.17 | 5.4 | 6.4 | 100 | 93 | 0.046 | 0.046 | 6.7 | 8.8 |
| NMI | 0.21 | 0.19 | 12.7 | 13.0 | 72 | 58 | 0.046 | 0.046 | 7.5 | 9.5 |
| ECC | 0.26 | 0.24 | 12.2 | 12.6 | 89 | 86 | 0.057 | 0.057 | 7.1 | 9.3 |
| H | 0.29 | 0.29 | 34.2 | 34.7 | 38 | 34 | 0.046 | 0.046 | 4.8 | 4.3 |
| PSMI | 0.22 | 0.29 | 34.1 | 34.3 | 50 | 40 | 0.046 | 0.046 | 1.8 | 1.6 |
| E | 0.29 | 0.29 | 33.2 | 34.0 | 46 | 37 | 0.046 | 0.046 | 5.9 | 5.2 |
| CoR | 0.14 | 0.14 | 6.2 | 7.4 | 92 | 84 | 0.046 | 0.057 | 8.8 | 11 |
| WC | 0.12 | 0 | 7.7 | 10.4 | 111 | 100 | 0.046 | 0.079 | 14 | 4.4 |

4.2. Rigid registration evaluation framework

Rigid registration SM has been globally evaluated using an optimization independent protocol proposed by Skerl. In this method the golden standard registration transform is known. The main idea of this protocol is to sample some position in a normalized parameter space around the gold standard. The performance of the SM is then estimated by some statistics of the SM computed on these positions. This protocol allows to estimate the accuracy (ACC) of the SM (the distance between the global maximum and the gold standard) and 4 other statistics related to the behavior of the SM during the optimization: the number of local minima (NOM); the capture range (CR) defined as the distance between the global maximum and the closest local minimum; the measure of distinctiveness (DO) defined as the average change of the SM near the global maximum; and the risk of non convergence (RON) which can be seen as the area of positions around the global maximum to which optimization may converge to local maxima.

4.3. Elastic registration evaluation framework

Elastic registration is difficult to evaluate because the same moving image can be obtained by applying different deformation fields on the same fixed image. So the direct evaluation by comparing an estimated deformation field to the gold standard one has no sense [13]. We only assess the influence of the SM on the registration accuracy using the following protocol. First, we estimated the deformation field between the simulated US and CT images using our elastic registration method. We applied then the estimated deformation field to the phantom image. Finally, the difference between this deformed phantom model and the gold standard phantom model is measured by computing the overlap of the several structures areas between both images by the Dice score.

$$Dice = \frac{2|A_1 \cap A_2|}{|A_1| + |A_2|} \quad (4)$$

with A_1 the structure surface in the gold standard phantom model and A_2 the structure surface in the deformed phantom image.

5. Results and discussion

Two registration cases has been studied: the registration of the simulated CT images with the corresponding raw US simulated images (denoted RI in the rest of the paper) and the CT images with the US images preprocessed as in [4] (denoted PI). The goal of the evaluation is to measure the impact of the several SMs on the rigid and on the elastic registration.

Rigid registration evaluation: The statistical results for the several SM using Skerl's protocol can be seen in Table 1. In this table the best values are bolded.

It can be observed in Table 1 that WC presents a globally better performance than the other SMs. This is especially true for the ACC, CR and DO indicators. MI and CoR equally give globally relatively high performances. Results show that MI can be used in the registration of CT to US images as it has been done in [4]. However, results also show that preprocessing the images does not improve the performance. If we compare the behavior between the raw and preprocessed images, it can be concluded that the performance is almost the same for all SMs except for WC which has a optimal ACC on the preprocessed images. All SMs have a small CR, as was expected for these modalities. This result is consistent with that reported in [14].

However a global comparison between the several SM is difficult to perform by the single analysis of Table 1. We propose to compute a composite index as a combination of the statistics for each SM. For this we used principal components analysis (PCA) for ranking the similarity measures. The coefficients of the first principal component give the composite index [15]. The coefficients of

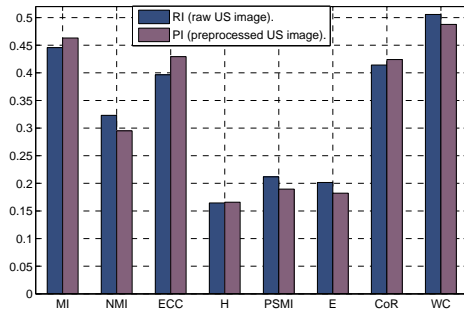


Figure 2. Composite index for the several SMs

the linear combinations of the properties that generate the principal components are shown in Figure 2. The largest coefficients in the first principal component are WC and MI for both RI and PI. However, the third is CoR for RI and ECC for PI.

Elastic registration evaluation: The elastic registration has been performed using the dedicated software Elastix [16]. According to our registration problematic this software proposes several transformations including B-splines. But the choice of SMs suited for multimodal registration supported by Elastix is only limited to MI and NMI. With this restriction the average Dice result for all LAPVs images indicates an overlap area of 93.02 percent for MI and of 97.08 percent for NMI using RI US images. With PI US images the results were: 94.17 percent for MI and 97.94 percent for NMI. These high scores confirm the validity of the elastic registration between US and CT images. For elastic registration NMI seems to be more efficient than MI. In addition, preprocessing US images improve the registration. However, the implementation of the others SMs especially WC or CoR into Elastix toolbox should be investigated.

5.1. Conclusions

The evaluation of CT to US images registration was performed for rigid and elastic transformations. The performance of different intensity based similarity measures was compared. The results validate the use of intensity measures to perform the registration between CT and US despite intensity representation in the images. For rigid registration, an optimization independent evaluation of eight intensity similarity measures was performed. The similarity measures WC and MI have the global better performance. For elastic registration, NMI show a slightly better accuracy result than MI when the registration was performed in Elastix software.

References

- [1] Cox JL. Atrial fibrillation II: rationale for surgical treatment. *J Thorac Cardiovasc Surg* 2003;126(6):1693–1699.
- [2] Pichardo S, Hynynen K. New design for an endoesophageal sector-based array for the treatment of atrial fibrillation: a parametric simulation study. *IEEE Trans Ultrason Ferroelectr Freq Control* 2009;56(3):600–612.
- [3] Huang X, et al. Dynamic 2D ultrasound and 3D CT image registration of the beating heart. *IEEE Trans Med Imaging* 2009;28(8):1179–1189.
- [4] Huang X, et al. Rapid registration of multimodal images using a reduced number of voxels. In *Proc. SPIE Med. Imag.* 2006; 1–10.
- [5] Unser M. Splines: A perfect fit for signal and image processing. *IEEE Signal Process Mag* 1999;16(6):22–38.
- [6] Maes F, et al. Multimodality image registration by maximization of mutual information. *IEEE Trans Med Imaging* 1997;16(2):187–198.
- [7] Studholme C, et al. An overlap invariant entropy measure of 3D medical image alignment. *Pattern Recognit* 1999; 32(1):71–86.
- [8] Rogelj P, et al. Point similarity measures for non-rigid registration of multi-modal data. *Compt Vis Image Und* 2003; 92(1):112–140.
- [9] Bro-Nielsen M. Rigid registration of CT, MR and cryosection images using a GLCM framework. In *Proc. CVRMed* 97. 1997; 171–180.
- [10] Roche A, et al. The correlation ratio as a new similarity measure for multimodal image registration. In *Proc. MIC-CAI98*. Springer, 1998; 1115–1124.
- [11] Woods RP, et al. MRI-PET registration with automated algorithm. *J Comput Assist Tomogr* 1993;17(4):536–546.
- [12] Dillenseger JL, et al. Fast simulation of ultrasound images from a CT volume. *Comput Biol Med* 2009;39(2):180–186.
- [13] Klein S, et al. Evaluation of optimization methods for non-rigid medical image registration using mutual information and B-splines. *IEEE Trans Im Proc* 2007;16(12):2879–2890.
- [14] Skerl D, et al. A protocol for evaluation of similarity measures for rigid registration. *IEEE Trans Med Imaging* 2006; 25(6):779–791.
- [15] Mishra S. On construction of robust composite indices by linear aggregation. *The IUP Journal of Computational Mathematics* 2009;2(3):24–44.
- [16] Klein S, et al. Elastix: a toolbox for intensity-based medical image registration. *IEEE Trans Med Imaging* 2010; 29(1):196–205.

Address for correspondence:

Zulma SANDOVAL
 Université de Rennes1, Campus de Beaulieu - Bat 22, cedex
 35042, Rennes, France.
 zulma.sandoval-betancur@etudiant.univ-rennes1.fr